Polymer chain in a flow through a porous medium: A Monte Carlo simulation

V. Yamakov* and A. Milchev
Institute for Physical Chemistry, Bulgarian Academy of Sciences, Georgi Bonchev Street, Block 11, 1113 Sofia, Bulgaria
(Received 19 February 1997; revised manuscript received 5 August 1997)

We study conformational and dynamic properties of dilute polymer solutions drifting through a random environment of obstacles at varying intensity of the external field B and of the host matrix density C_{ob} using dynamic Monte Carlo simulation of an off-lattice bead-spring model. The presence of obstacles is found to influence strongly the conformational properties of the drifting chains: with growing strength of the field B and $C_{\mathrm{ob}}=0$ the chain mean size (gyration radius), R_g^2, rapidly increases while the ratio between the end-to-end distance, R_{ee}^2, and R_g^2 drops essentially below the usual value of 6, typical in the absence of drift, suggesting a hooflike shape of the chain with both ends directed along the external field vector. We confirm the finding of G. M. Foo and R. B. Pandey [Phys. Rev. E **51**, 5738 (1995)] of a critical strength of the external field B_c above which the permeability of the host matrix sharply drops. A detailed study of this phenomenon suggests that B_c may be related to a dramatic growth of a specific ''capture'' time, characterizing the interaction of the chains with the obstacles, so that a simple model describing the drift of chains among obstacles may be shown to reproduce our findings. [S1063-651X(97)10912-6]

PACS number(s): 36.20.−r, 82.45.+z, 87.15.−v

I. INTRODUCTION

In a previous publication, [1] a scaling analysis of chain conformations, diffusivity, and characteristic relaxation times of a polymer in a porous medium was suggested in order to interpret the influence of a random environment on the static and dynamic properties of the macromolecule. A natural extension of these investigations would be the study of the drift of a polymer chain through a porous medium, caused by external field (bias). This problem is closely related to ion and mass transport in complex polymer mixtures, molecular permeation in gels (electrophoresis), sedimentation studies, marine geosciences, water flooding in secondary oil recovery, etc., and has been the subject of considerable interest in recent years [2]; it has been addressed by experimental [3–12], theoretical [2,13–15], and simulational [13,16–19] studies on this subject.

The non-Newtonian behavior of a polymer solution [20,21] is an essential property to investigate. Experimental measurements [3,11] reveal that above a certain velocity a very dilute polymer solution, driven through cavities of packed beads, shows a non-Newtonian behavior manifested by an anomalous increase of the friction factor f of the medium with increasing flow velocity. This, observed also by Vissmann and Bewersdorff [10], is interpreted as being due to an interaction between extension and shear deformations and may be attributed to the dominance of extension stress [3].

Theoretical observations based on dumbbell models, e.g., by either a ''linear'' one with a Hookean spring connector force between the two beads, or by a nonlinear FENE (finitely extendable nonlinear elastic) connecting potential, show [2,15] stretching of the polymers during flow in porous media. The Hookean spring model in a strong flow and dense environment even predicts a catastrophic situation of permanent growth of the gyration radius to infinity. The numerical calculations performed by Chilcott and Rallison [13] for a suspension of FENE dumbbells, passing cylindrical and spherical surfaces, revealed that the nonlinear part of the FENE potential limits the growth of the dumbbell link to a large fraction of its maximum extensibility. Several models for the stretching conformations of polymers in extensional flows based on experimental [6,7] and theoretical [16,17,22] studies are known in the literature.

In order to overcome experimental difficulties as well as avoid severe approximations in the analytical treatment, computer simulations could appear to be especially suited as a means to get more insight into the complexity of the problem. An attempt [18,19] to simulate polymers driven through a porous medium in two dimensions, using a reptational Monte Carlo technique, confirmed the expected growth of the gyration radius with increasing drift rate. However, these studies reported a decrease of the growth with increasing density of the porous medium [19], contrary to the expected theoretical predictions, cited above. These simulations of the permeability of the media in dependence of the drift rates confirmed also the experimentally observed [3,11] decrease of the permeability above some critical flow rate, characteristic for the system, albeit no interpretation of these results has been suggested. Given that the applicability of reptational algorithms to nonequilibrium studies of polymers is questionable in principle, it was clear that more studies are needed so that a comprehensive understanding of the properties of polymer drift through porous media is achieved.

In this paper we report simulation results, based on an off-lattice bead-spring model of a polymer chain [23], placed in a three-dimensional random medium of obstacles, studied by a dynamic Monte Carlo simulation technique. The model has been used before in a number of studies of polymer solutions in the bulk [24], at interfaces [25], in constrained geometries [26], etc., and is known to reproduce faithfully

*Present address: Max-Planck-Institut fur Polymerforschung, Ackermannweg 10, D55021 Mainz, Germany. Electronic address: yamakov@ipchp.ipc.acad.bg

the static properties and the Rouse dynamics of long macromolecules with excluded volume interactions. Although the model does not consider hydrodynamic interactions between molecules or the inhomogeneity of the flow of the solvent around the introduced obstacles, as done in some theoretical studies [17,22], it reproduces chain conformations, similar to those predicted by these works.

As in our previous paper [1], in the present investigation we use as a host matrix an equilibrated dense solution of identical polymer chains that is frozen at different concentrations $C_{\rm ob}$. We then let a single chain (or a small number of noninteracting chains), driven by an external (bias) field B, move through these realizations of the random media. The simulational procedure is briefly explained in Sec. II. A brief analysis of the measured quantities at the long-time regime is made in Sec. III. The conformational properties of a driven chain through a random medium are then presented and discussed in Sec. IV where they are shown to agree well with the quoted theoretical and experimental observations. In Sec. V we focus on the mobility of the chain at different drift rates, demonstrating its non-Newtonian behavior at high drift velocity. We also suggest a simple phenomenological interpretation of our findings. Results for the longitudinal and lateral components of the effective diffusivity, as introduced by Saffman [27] for a flow of a dynamically neutral material through a porous medium, are then presented in Sec. VI. We conclude our report in Sec. VII with a brief summary of our observations and conclusions.

II. THE MODEL

In our off-lattice bead-spring model of a polymer chain [23,1], placed in a random medium of obstacles, one deals with N ''effective monomers,'' connected by springs, representing ''effective bonds,'' using a FENE potential:

$$U_{\rm FENE}(r) = \begin{cases} -\frac{k}{2}R^2\ln\left[1-\left(\frac{r-l_0}{R}\right)^2\right], & \text{for } l_0-R<r<l_0+R, \\ \infty, & \text{otherwise,} \end{cases} \tag{1}$$

where r is the distance between two successive beads, $l_0=0.7$ is the unperturbed bond length, $R=l_{\rm max}-l_0=0.3$, and $k/2=20$ (in our units of energy $k_BT=1.0$) is the elastic constant of the FENE potential, which behaves as a harmonic potential for $r-l_0 \ll R$, that is, $U_{\rm FENE}(r\approx l_0)\approx -(k/2)(r-l_0)^2$ but diverges logarithmically for both $r\to l_{\rm max}$ and $r\to l_{\rm min}=2l_0-l_{\rm max}$. We choose our unit of length such that $l_{\rm max}=1$ and then $l_{\rm min}=0.4$.

The nonbonded interaction is described by a Morse potential,

$$U_M(r)=\epsilon_M\{\exp[-2a(r-r_{\rm min})]-2\exp[-a(r-r_{\rm min})]\} \quad \text{for } 0<r<\infty, \tag{2}$$

where $r_{\rm min}=0.8$, $\epsilon_M=1$, and the large value of $a=24$ makes interactions vanish at distances larger than unity, so that an efficient *link-cell* algorithm [23] for short-range interactions can be implemented.

The radius of the beads and the interactions, Eqs. (1), (2), have been chosen such that the chains may not intersect themselves or each other in the course of their movement within the box.

A standard Metropolis algorithm is used, whereby an attempted move of a randomly selected particle in a random direction $\Delta x,\Delta y,\Delta z$ is accepted with probability, equal to

$$P=\begin{cases} \exp[-(E_{\rm new}-B\Delta x-E_{\rm old})/k_BT] & \text{for } E_{\rm new}-B\Delta x>E_{\rm old}, \\ 1, & \text{otherwise,} \end{cases} \tag{3}$$

where $E_{\rm new}$ and $E_{\rm old}$ are the energies of the new and old system configurations. The external field, or bias, B, is introduced in the system as an additional term in the Boltzmann probability in Eq. (3) where Δx denotes the attempted move distance in the x direction, which is the direction of the bias field too.

The porous medium is the same as in our previous paper [1]. It consists of an initially relaxed and then frozen network of polymer chains of length $N=16$, and the monomers have the same size as those of the diffusing chain. The concentration of the network $C_{\rm ob}$ is varied and the behavior of diffusing chains of various length N at various drift rates B is studied in the good solvent regime, $k_BT=1.0$, since from previous studies of the model it is known that the θ temperature $k_BT_\theta=0.62$ [24].

The static properties of the chains are studied by measuring their mean square radius of gyration R_g^2,

$$R_g^2=\frac{1}{N}\sum_{n=1}^{N}\langle(r_n-r_{\rm c.m.})^2\rangle, \tag{4}$$

where

$$r_{\rm c.m.}=\frac{1}{N}\sum_{n=1}^{N} r_n \tag{5}$$

and r_n is the radius vector of the nth bead of the chain.

In addition to the conventional mean square displacements of the middle monomers g_1,g_2, in an absolute- and in a center-of-mass coordinate system, and of the center of gravity of the chains, g_3, used in previous investigations [23,1],

$$g_1(t)=\langle[r_{N/2}(t)-r_{N/2}(0)]^2\rangle,$$

$$g_2(t)=\langle\{[r_{N/2}(t)-r_{\text{c.m.}}(t)]-[r_{N/2}(0)-r_{\text{c.m.}}(0)]\}^2\rangle,$$

$$g_3(t)=\langle[r_{\text{c.m.}}(t)-r_{\text{c.m.}}(0)]^2\rangle, \tag{6}$$

we define here several mean square displacements, relative to the *total* center of mass of the polymer fluid, $R_{\text{c.m.}}$,

$$g_{1\_\text{c.m.}}(t)=\langle\{[r_{N/2}(t)-R_{\text{c.m.}}(t)]-[r_{N/2}(0)-R_{\text{c.m.}}(0)]\}^2\rangle,$$

$$g_{3\_\text{c.m.}}(t)=\langle\{[r_{\text{c.m.}}(t)-R_{\text{c.m.}}(t)]-[r_{\text{c.m.}}(0)-R_{\text{c.m.}}(0)]\}^2\rangle, \tag{7}$$

consisting of many noninteracting (interpenetrable) chains (each driven polymer in the system does not ''feel'' the other driven polymers and can penetrate through them). In the presence of an external field the chain drifts through the medium and the mean square displacement of its center of mass is a quadratic function of time [measured in Monte Carlo steps (MCS) per monomer (bead), whereby 1 MCS is the time needed for all monomers to perform an attempted move $\Delta x,\Delta y,\Delta z\leqslant\pm 0.5$ in a random direction]. Thus $g_3(t)$ from Eq. (6) yields the average velocity of a chain:

$$V_N^2=\lim_{t\to\infty}[g_3(t)/t^2]. \tag{8}$$

In the long-time limit V_N must coincide with the average velocity of the total mass center of the fluid, defined as

$$V_{\text{c.m.}}^2=\lim_{t\to\infty}[R_{\text{c.m.}}^2(t)/t^2]. \tag{9}$$

The difference between V_N and $V_{\text{c.m.}}$ may serve as a control parameter for the statistics of our measurements.

Similarly to the case of a system without bias, a definition for the so-called *effective diffusivity* [27] can be introduced using the ratio of the relative mean-square displacement of the center of gravity of a single chain $g_{3\_\text{c.m.}}(t)$ with respect to time t:

$$6D_{\text{eff}}=\lim_{t\to\infty}[g_{3\_\text{c.m.}}(t)/t]. \tag{10}$$

With the various types of displacements, introduced above, a number of characteristic relaxation times, $\tau_{1\_\text{c.m.}}$, τ_2, $\tau_{3\_\text{c.m.}}$, can be defined:

$$g_{1\_\text{c.m.}}(\tau_{1\_\text{c.m.}})=\langle R_g^2\rangle,\quad g_2(\tau_2)=\tfrac{1}{3}\langle R_g^2\rangle,$$

$$g_{3\_\text{c.m.}}(\tau_{3\_\text{c.m.}})=g_2(\tau_{3\_\text{c.m.}}). \tag{11}$$

The index $_{\text{c.m.}}$ of $\tau_{1\_\text{c.m.}}$ and $\tau_{3\_\text{c.m.}}$ stands for the fact that they are calculated in a moving coordinate system connected with $R_{\text{c.m.}}$, at variance with their conventional definition [28,1]. The definition of τ_2 is also slightly modified by using a different prefactor 1/3 instead of 2/3 [28,1] because of the non-Gaussian elongated conformation of the chains in a flow. This does not change the principal behavior of τ_2 but only decreases its time scale so that better statistics can be used in its determination.

The simulations have been performed in a volume of 32^3 effective cells of size 1 using periodic boundary conditions,

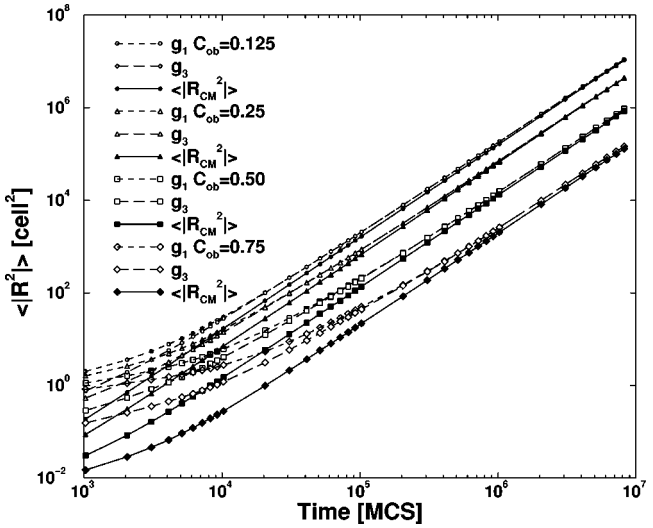

FIG. 1. Mean square displacements of the central bead g_1, center of mass g_3 of a polymer chain, and the center of mass of the whole polymer fluid $R_{\text{c.m.}}^2$ vs time for $N=32$ and $B=0.25$ for a series of densities C_{ob} of the host matrix.

and in the highest concentration regime they contain up to 24 576 fixed monomers in 1536 chains of length $N=16$ that form the porous media. The diffusing chains, immersed into this host matrix, have been chosen with lengths of 8, 16, and 32 monomers. The intensity of the external field B is varied from 0.0625 to 1.5 relative units (in our case *energy* in k_BT per *distance* in unit lengths). To obtain better statistics we performed three independent measurements for each random media, changing the direction of the field along the x, y, and z axes, and then averaged the results.

III. LONG-TIME REGIME

All our results and analysis presented in this paper concern the long-time behavior of the chains drifting through the porous medium in a sense that all measured quantities have already reached their long-time asymptotic limits. To reach and explore these limits for each system we used four sequential runs of 10^7 MCS each (the final configuration of a given run becomes a starting configuration for the next one) and the measurements were performed at every 10^3 MCS starting from the second run after the system has been equilibrated for 10^7 MCS.

In Fig. 1 one can verify that the mean-square displacements of the longest chains ($N=32$) studied, g_1, g_3, and $R_{\text{c.m.}}^2$ coincide well at times 10^6–10^7 MCS for all densities of the host matrix at $B<B_c\approx 0.25$ (see below). Note that the value of these displacements goes up to 10^5–10^7 square cell units, which, compared to chain size $R_g^2=6.3$ (Fig. 8), means that the polymers have traveled a distance of $(10^2-10^3)R_g$ during the MC simulations and the long-time regime of drift has been successfully reached. As long as the travel distance is between 10 and 10^2 box sizes, the data might be influenced by certain finite-size effects. Such effects are difficult to estimate in our model since their high computational efficiency is based on bitwise operations so that most quantities, such as the box size and the chain length, must be multiples of two. Thus the next box size of 64^3 cubic cells would

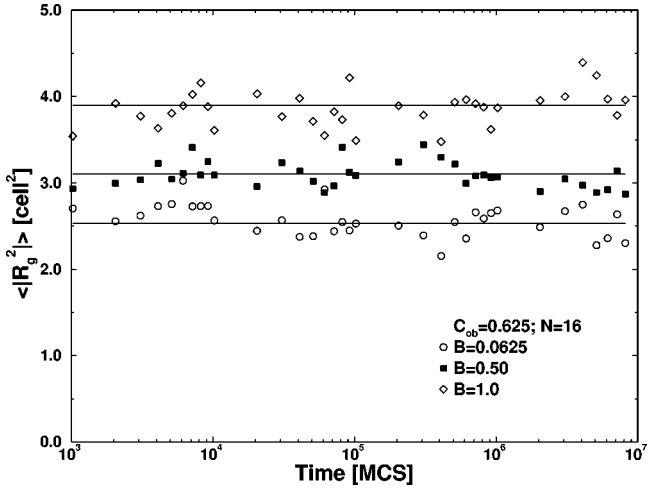

FIG. 2. Instantaneous values of the mean-square gyration radius at different times during a simulational run. The measured values are averages over 16 chains of $N=16$ at three sequential runs of 10^7 MCS. The measurements were performed after an initial period of 10^7 MCS has elapsed. The straight horizontal lines mark the average values of all the measurements, performed periodically every 10^3 MCS (not all of them are shown on the figure).

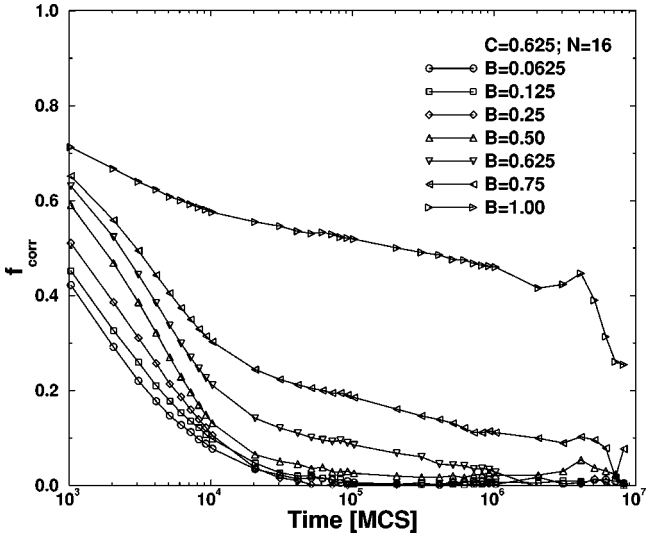

FIG. 3. Correlation functions of the end-to-end chain distance for the systems from Fig. 2.

accommodate 8 times more particles at the same density of the medium and would exceed the operational memory of a modern RISC Work station computer. We have tried therefore to allow for such finite-size effects by changing the host matrix and the direction of the bias field during simulations.

The long-time steady state variation of conformational quantities such as the radius of gyration is demonstrated in Fig. 2 for one of the highest obstacle concentrations $C_{\rm ob}=0.625$ in a very long time interval. Even at the strongest field, $B=1.0$, we do not detect any systematic drift of the instantaneous values of R_g^2 with time. The straight lines mark the average values of all the measurements every 10^3 MCS (not all are shown on the figure). The data at a very weak bias $B=0.0625$ are given for comparison.

The length of the time intervals of 10^7 MCS, used in the simulation, can be assessed by studying the time correlation between system configurations, for instance, of the end-to-end chain distance, defined as

$$R_{\rm corr}(t_i)=\frac{[1/(\mathcal{N}-i)](1/\mathcal{P})\sum_{j=1}^{\mathcal{N}-i}\sum_{\alpha=1}^{\mathcal{P}}(R_{j\alpha}-\langle R\rangle)(R_{j+i,\alpha}-\langle R\rangle)}{(1/\mathcal{N})(1/\mathcal{P})\sum_{j=1}^{\mathcal{N}}\sum_{\alpha=1}^{\mathcal{P}}(R_{j\alpha}-\langle R\rangle)^2}, \tag{12}$$

where $R_{j\alpha}$ is the end-to-end distance of the α chain, measured at time t_j,

$$R_{j\alpha}=\sqrt{[r_N(t_j,\alpha)-r_1(t_j,\alpha)]^2} \tag{13}$$

and $\langle R\rangle$ is its mean value, averaged over all measurements $\mathcal{N}$ and number chains $\mathcal{P}$.

The results for the systems shown in Fig. 2 are presented in Fig. 3. For the cases of $B<B_c$ (for $N=16$ $B_c\approx 0.5$ as will be shown below) the configurations after times $t>10^5$ do not correlate practically. For $B>B_c$, however, the time needed to reach a new uncorrelated configuration rises exponentially, and for $B=1.0$ even 10^7 MCS are not enough to obtain a completely independent configuration.

Thus one may claim that for $B<B_c$ we have reached the long-time steady-state regime for all of the data presented below. Our analysis concerns mainly this regime, although we give some results and a possible interpretation of the behavior of the chains even beyond $B\approx B_c$, assuming that the measured quantities are not very far from their equilibrium values, as can be seen from Figs. 1 and 2.

IV. CONFORMATIONAL PROPERTIES OF A CHAIN DRIVEN THROUGH POROUS MEDIA

In a three-dimensional (3D) plot in Fig. 4(a) we show the variation of $\langle R_g^2\rangle$ of a driven chain through porous media with increasing external field B at different densities $C_{\rm ob}$ of the medium. While in the absence of obstacles, $C_{\rm ob}=0$, no dependence of the gyration radius on the field B is observed, as it should be, even a slight inclusion, $C_{\rm ob}=0.125$, of fixed particles in the system leads to a significant increase of the size of the chains at higher drift rates ($B>0.5$). The ratio between longitudinal $\langle R_{gl}^2\rangle$ and transversal $\langle R_{gt}^2\rangle$ components, plotted in Fig. 4(b), indicates that this increase is

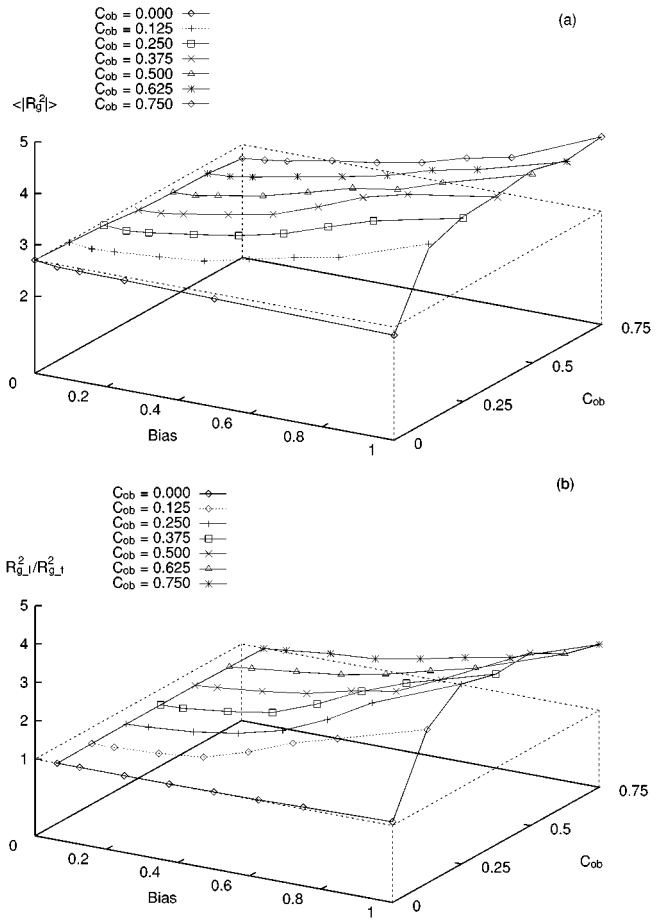

FIG. 4. (a) Mean-square gyration radius R_g^2 measured in the way presented in Fig. 2 and (b) the ratio of its longitudinal and transversal components $\langle R_{gl}^2\rangle/\langle R_{gt}^2\rangle$ vs bias for a series of densities $C_{\rm ob}$ of the host matrix.

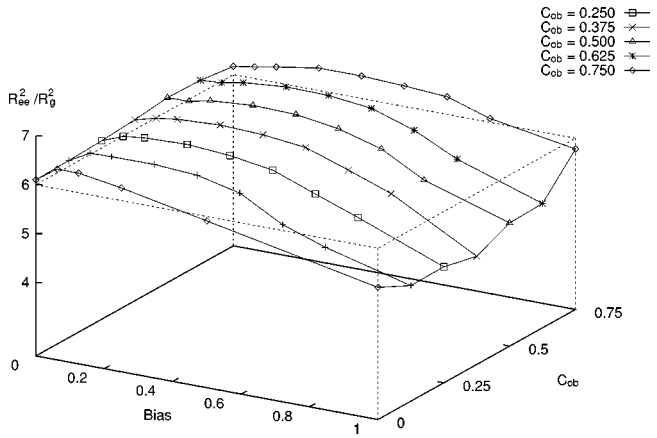

FIG. 5. The ratio between the end-to-end mean-square distance and the mean-square gyration radius $\langle R_{ee}^2\rangle/\langle R_g^2\rangle$ vs bias for series of densities $C_{\rm ob}$ of the host matrix.

mainly due to stretching of the polymer along the drift direction. If such a stretching is assumed, one must then expect an increase of the ratio $\langle R_{ee}^2\rangle/\langle R_g^2\rangle$, where $\langle R_{ee}^2\rangle$ is the mean square end-to-end distance, in comparison with that of a chain in free space. For a Gaussian coil its theoretical value is 6, while for a stretched linear string it is 12. However, in Fig. 5 one can clearly see that after a slight increase of up to 6.4, a decrease of $\langle R_{ee}^2\rangle/\langle R_g^2\rangle$ with increasing B takes place, the ratio going down to values even below 5 at intermediate matrix density $C_{\rm ob}=0.25$–0.50. This effect is weakened at high obstacle concentrations $C_{\rm ob}=0.75$ because at these densities the conformation of the diffusing chain is governed strongly by the configuration of the pores in the medium [1]. A simple explanation of this decreasing ratio is to assume a hooflike form of the chain with ends directed along the drift (Fig. 6), so that the two end beads get closer to one another as they are more mobile than the inner beads, the latter being frequently hooked in the presence of obstacles. This is observed even for a chain driven in free space, as one can notice in Fig. 5 for $C_{\rm ob}=0$. Of course, one can attribute this to finite-size effects and can expect that in the limit of infinitely long chains this decline of $\langle R_{ee}^2\rangle/\langle R_g^2\rangle$ should not be observed. Because we were forced to limit our simulations to chain lengths of 32 beads, however, we were not able to check this during the present study.

It is interesting to note that the typical conformations of the chains, usually observed in our simulations (Fig. 6), are similar to those reported for polymers in extensional flows [6,7,16,17,22], in spite of the fact that we do not consider any inhomogeneity of the flow of the solvent, modeled by the biased field ($B=$const everywhere in the system) in between the obstacles. This unexpected similarity may be due to the fact that the acceptance rate in the simulations is different away from an obstacle and close to it—in a space free

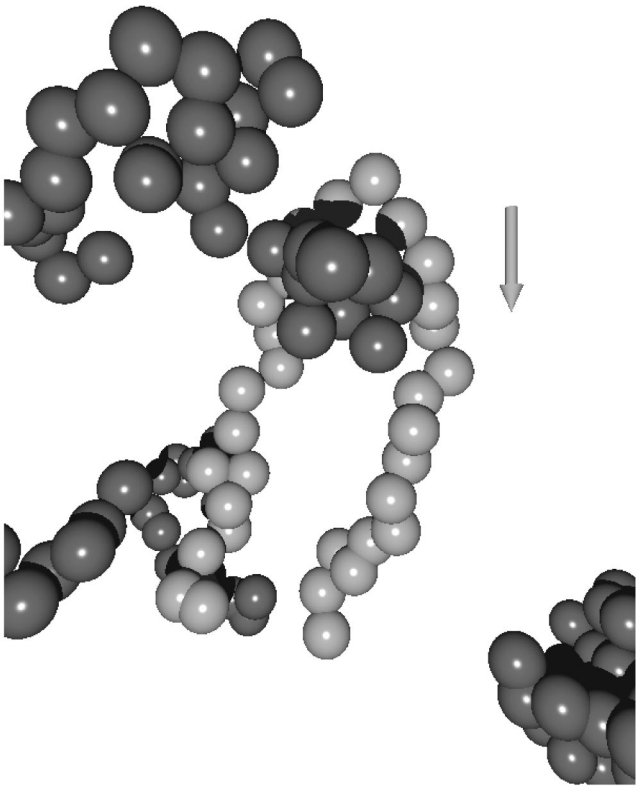

FIG. 6. A snapshot of a typical hooflike form of a driven 32 beads chain (light beads) at overcritical bias $B=0.625$ through a dilute medium of obstacles (dark beads) of density $C_{\rm ob}=0.125$. The direction of the drift is indicated by the arrow.

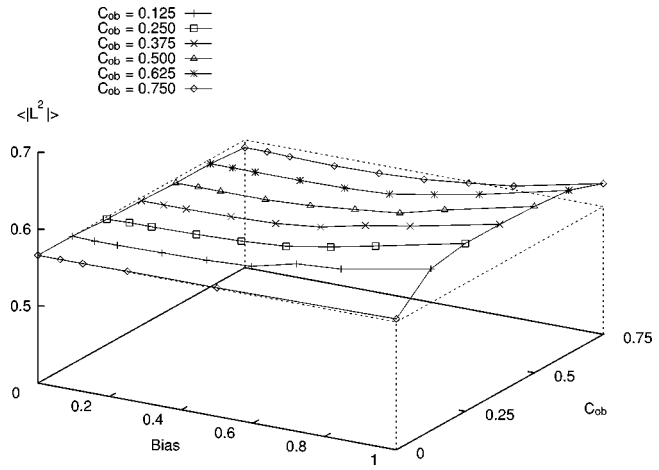

FIG. 7. Average square bond length $\langle l^2 \rangle$, measured in square cell unit length, vs bias B for a series of densities $C_{\rm ob}$ of the host matrix.

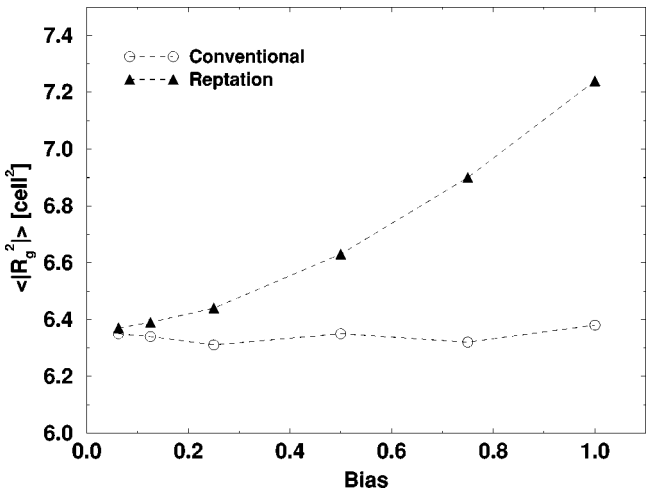

FIG. 8. Mean-square gyration radius R_g^2 calculated in the absence of obstacles by means of conventional Monte Carlo technique (open circles) and using a reptational Monte Carlo algorithm (filled triangles).

of obstacles the acceptance rate can be 10 or more times larger than that in a dense system. This introduces a kind of inhomogeneity in the dynamics of the system, similar to that caused by extensional flow. An original kink model for unraveling of a polymer chain in a strong extensional flow is presented by Larson [17]. He states that the increasing of the extensional flow decreases the number of kinks along the chain, thus straightening it along the flow. An earlier theoretical analysis, done by Ryskin [22], who refers to the experimental results of James and Saringer [6], reveals that such unraveling starts at the middle and spreads throughout the ends of the chain, thus forming a ''coil-string-coil'' picture. Ryskin argues that this model is favored by the well-known experimental fact [29] that the chain scission in shear degradation occurs almost precisely at the midpoint of the chain. The typical chain conformation that we observe at high bias is a good example of the ''coil-string-coil'' model. In Fig. 6 one can notice that the driven polymer is more coiled at the ends as compared to the middle part, where it is completely stretched.

The predicted elongation of the average square bond length $\langle l^2 \rangle$, based on a dumbbell model with FENE potential between the beads [2,13,15], is also confirmed in our simulations as seen from Fig. 7. Again we should point out that extensions of the bonds occur for sufficiently strong fields, B, and predominantly in the intermediate range of obstacle densities.

At this point it should also be noted that our results for the conformation of a driven chain disagree with the earlier findings of Foo and Pandey [19], as has been already mentioned in the Introduction. The main difference is in the behavior of the observed rate of conformational elongation of the driven chain with increasing of the obstacle concentration. While our results (in agreement with the cited theoretical analysis) show a definite increase of the elongation with increasing the media density [Fig. 4(a)] and no change of $\langle R_g^2 \rangle$ with B in the absence of obstacles, the results of Foo and Pandey [19] show maximal elongation of the driven chain in the free space, which then rapidly decreases with increasing the obstacle density. Our analysis of this point shows that the behavior observed by Foo and Pandey [19] is an artifact of the reptational algorithm, which they use in their study. In a reptational algorithm one moves the two end beads of the chain only, which are thus more mobile and, in the presence of a bias field, stretch their bonds much more than the inner beads do. In the process of reptation the end monomers become inner monomers and these elongated bonds become bonds inside the chain. Thus after a short time ($\propto N^2$) all the bonds of the chain will be abnormally elongated, which will affect the size of the coil as a whole. We performed a test applying reptational algorithm in comparison to the conventional one where *all* the monomers are moved in a random manner. Our results for $\langle R_g^2 \rangle$ with the reptational algorithm reproduce those reported by Foo and Pandey [19]. In Fig. 8 we plot the $\langle R_g^2 \rangle$ vs B relationship in free space (as there the difference is most obvious). Evidently, while the conventional algorithm produces no dependence of the chain size on B within the range of statistical errors, the reptational algorithm shows a systematic increase of the chain size with the bias B.

Thus our conclusion is that the reptational algorithm is not applicable for the simulation of systems in a drift, because it affects in a wrong way not only the dynamic, but also the *static* properties of the driven macromolecules, in contrast to the case of equilibrium polymer systems, where the reptational algorithm does not affect the static properties.

V. MOBILITY OF A POLYMER CHAIN DRIVEN THROUGH A POROUS MEDIUM

In the case of a slow drift through a dilute porous medium, when the conformation of the driven chain is not affected essentially by the drift, the average velocity of the molecule is a linear function of the mobility μ of the chain and the total external force $f_{\rm tot}$ acting on it [30], which in our case is BN:

$$V_N = \mu f_{\rm tot} = \mu BN. \tag{14}$$

Applying Einstein's formula, which links μ with the diffusion coefficient D_N,

$$D_N = \mu k_B T, \tag{15}$$

we obtain a relation for the average velocity as a function of the diffusion coefficient and the bias:

$$V_0 = D_0 BN/k_B T. \tag{16}$$

Here the index 0 at D denotes the diffusion coefficient, measured when no external field is applied, $B=0$, and V_0 stands for a ''zero'' approximation, i.e., this relation is applicable only for slow drift in a dilute medium.

The simulation data, represented in Figs. 9(a)–9(c) confirm Eq. (16) in the region of weak $f_{\rm tot}$ ($BN<4$, for $N=8,16,32$) at dilute regimes. The straight lines drawn through the origin of the coordinate system in Figs. 9(a)–9(c) indicate the exact relation in Eq. (16) with D_0, having the values of D_0 measured for the same systems without an external field [1]. A very good agreement of these lines with the measured data is observed for all the chain lengths in dilute media. Substantial discrepancies are seen only at high density of the porous medium. The regions of linearity of $V_N(B)$ correlate clearly with the regions of minor conformational deformations of the chain [see Figs. 4(a) and 4(b)].

For intermediate drift rates ($4<BN<8$), when the chain conformation starts to differ significantly from its equilibrium form [Figs. 4(a) and 4(b)], we observe a weaker than linear dependence of V_N on B. At even higher external fields ($BN>8$) $V_N(B)$ goes through a maximum at a critical value B_c of the field, calculated by means of a third-power polynomial interpolation of the data [dashed lines in Figs. 9(a)–9(c)], and then gradually decreases, as has been found earlier by Pandey [18,19].

Below we try to analyze this behavior in more detail. First, it is clearly seen [Figs. 9(a)–9(c)] that the critical bias B_c, at which the velocity starts to decrease, does not or very slightly depends on the obstacle concentration $C_{\rm ob}$. It turns out that B_c is reciprocal to the chain length N and one can readily show that for all chain lengths studied in this work ($N=8,16,32$), $NB_c=$const:

$$B_c N = f_c \approx 9. \tag{17}$$

Consequently, when the *total* force, acting upon the whole driven molecule, exceeds a certain well-defined value, which does not depend on the size of the molecule, the mobility of the polymer starts to decrease.

One could assume that this characteristic behavior of the chain mobility as a function of the bias is reflected by the typical relaxation times of the driven chain too. In Fig. 10 the variation of the relaxation time τ_2 from Eq. (11), reflecting the mobility of an inner monomer relative to the center of mass of the molecule, is presented for a dilute system as a function of B. Note that while for $B<B_c$ τ_2 is nearly constant (or rises very slowly), for $B \geqslant B_c$ it starts to rise dramatically. This effect is rapidly enhanced with growing length N of the chains. Thus at and above B_c the inner monomers of the molecule need an extremely long time until they start to move with the total chain as a whole, and this is matched by a decrease of the average chain velocity.

In order to explain this behavior, the following model for a dilute system is presented. Consider a very dilute system of obstacles among which a polymer is driven by an external

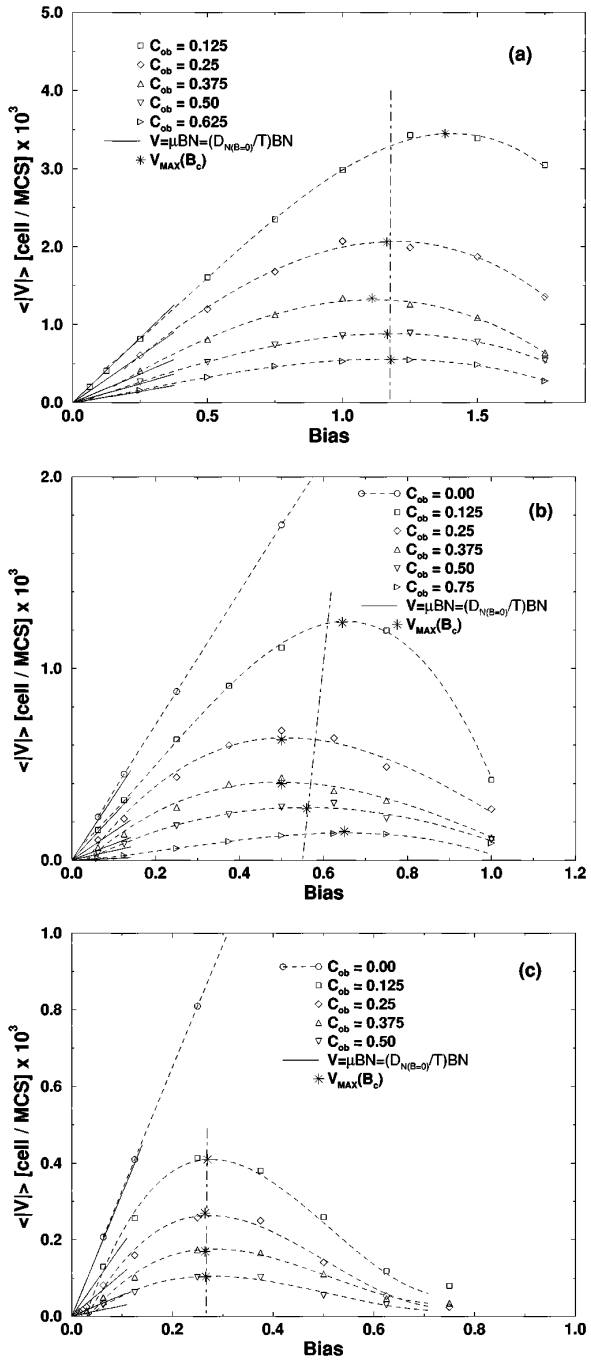

FIG. 9. Drift mean velocity of polymer chains of length (a) $N=8$, (b) $N=16$, and (c) $N=32$ vs bias B for a series of densities $C_{\rm ob}$ of the host matrix. The vertical long-dashed line on each of the figures indicates the approximate value of the critical bias B_c for the given chain length N. Velocity is given in unit length per MCS. The straight lines drawn through the origin of the coordinate system present the linear approximation of the velocity as given by Eq. (16) in the text.

force field. At small drift rates, when the deformation of the chain is negligible, the Einstein equation (15), determining the linear dependence of $V_N(BN)$, Eq. (16), is valid. This is an approximation where the effects of interaction between the polymer and the obstacles are not accounted for. In fact the motion of a chain molecule through a dilute system, $C_{\rm ob} \ll C^*$, of immobile obstacles can be divided into two

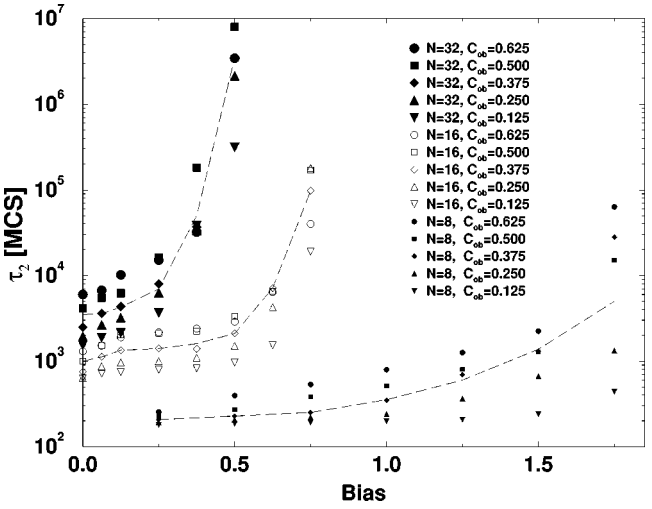

FIG. 10. Log-normal plot of relaxation time τ_2, Eq. (9) vs bias for three different chain lengths (given as a parameter) and a series of densities C_{ob} of the host matrix.

parts: (i) free motion from one obstacle to another, and (ii) interaction of the molecule with the next obstacle. We can express this analytically in the following way:

$$V_N=\frac{\xi}{\tau+t}, \tag{18}$$

where ξ is the average distance between the obstacles (the mean free path of the driven chain), t is the time needed for the polymer to travel this distance, which is equal to $t=\xi/V_0=\xi k_BT/D_0BN$, and τ is the time needed for the polymer to circumvent the obstacle (capture time). At drift rates below the critical bias, one can assume that τ does not depend on B (see Fig. 10) and by inserting t into Eq. (18) one can get the next approximation V_1 for the velocity

$$V_1=\frac{\xi D_0BN}{\tau D_0BN+\xi k_bT}. \tag{19}$$

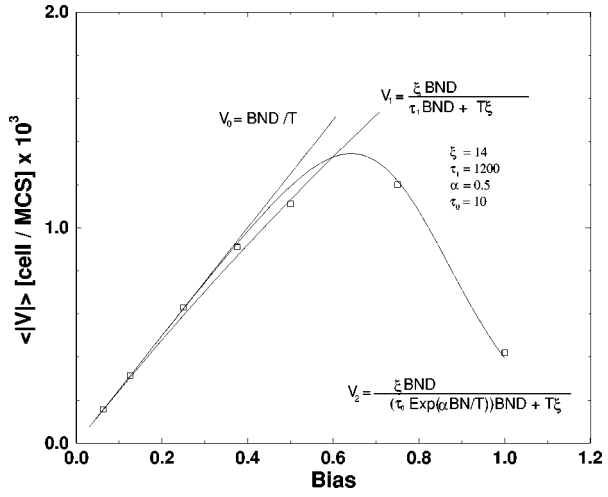

FIG. 11. Drift mean velocity, given in unit length per MCS, of chains of length $N=16$ at small obstacle concentration $C_{\mathrm{ob}}=0.125$ vs. bias B fitted with the expressions $V_0(BN)$, $V_1(BN)$, and $V_2(BN)$.

In Fig. 11 we have plotted the measured values of the average velocity of polymer chains with $N=16$, drifting through a dilute medium of obstacles, $C_{\mathrm{ob}}=0.125$, and we have approximated the data first with Eq. (16), which describes well the slow drift region and then Eq. (19) is applied with fitted parameters ξ and τ. It is seen that for reasonable values of ξ and τ we obtain a good agreement with the measured data nearly up to the characteristic maximum. The obtained fitted value for τ is of the order of the relaxation time τ_1, defined and measured as in our previous work [1] as

$$g_1(\tau_1)=\langle R_g^2\rangle. \tag{20}$$

This is the time needed for an inner monomer to travel a distance equal to the gyration radius of the polymer when no bias is applied. Note that for the present system, the size of the driven polymer is of the size of the frozen polymers, so that in this particular case τ_1 is approximately the time needed for the middle parts of the chain to bypass the obstacle in the course of their Brownian motion. For other systems we must add a prefactor to τ_1, which will not change the type of the relation in principle.

Because Eq. (19) provides no maximum, it cannot explain the slowing down of the chain at higher drift rates.

A maximum naturally appears, however, if one considers the process in which a driven chain overcomes some fixed obstacle as a thermally activated transition of the chain from a ''bound'' state into a state of free (drift) motion. The typical time required for such a process is then expected to be $\tau\propto\tau_0\exp(\Delta F/k_BT)$ where ΔF is the free energy difference of both states. ΔF is expected to be determined by the work needed to transform the conformation of a freely drifting chain into a stretched conformation of a chain hooked at an obstacle, that is, by the total force $f_{\mathrm{tot}}=BN$ acting over some finite displacement of the monomers, α.

$$V_2=\frac{\xi D_0BN}{[\tau_0\exp(\alpha BN/k_BT)]D_0BN+\xi k_BT}, \tag{21}$$

where τ_0 and α are parameters (Fig. 11).

Another possibility is to insert for τ in Eq. (19) the estimated values for τ_2 multiplied by a fitted prefactor, because the factor 1/3 in the definition of τ_2 in Eq. (11) has been arbitrarily chosen. However, due to the extremely steep rise of τ_2 at above critical field B_c, where its measurement is very difficult and inaccurate, we prefer here to use an approximation in the form of Eq. (21).

An explanation for the rapid increase of the capture time τ can be given by the following illustrative model. At weak external fields, when the force, acting upon a driven molecule, is below the critical value [Eq. (17)], the interaction with an immobile obstacle (which is a frozen polymer) should resemble an elastic collision of hard spheres. The driven chain does not penetrate into the inner space of the frozen chain, so τ is small. When the external field increases and the total force acting on the polymer reaches the critical value f_c, the incident polymer chain has enough power to overcome the entropic barrier and hook on the frozen chain. The two chains may entangle themselves and it becomes much more difficult for the driven one to get free again, so that τ rises.

Although the present model considers very dilute systems, it happens that the fit, based on Eq. (21), works well even at intermediate obstacle densities (up to $C=0.5$), if instead of the diffusion coefficient D_0, we use an effective one, calculated from the slope of the $V_N(BN)$ curve [Eq. (16)] at weak fields, which is slightly higher than D_0. Of course, at very weak bias this slope should attain the value of D_0, but our measurements for denser systems show that there is a slight increase in the mobility with growing bias. At this stage we do not study this in detail because in a dense system the interaction of the driven molecule with the host matrix is much more complex and we have to allow for a crossover of the chain dynamics to a reptational one, which is beyond the scope of the present study.

We should point out also that the entanglement of the driven polymer chains with the obstacles cannot explain the experimentally observed similar effect of non-Newtonian increase of the friction factor of a polymer flow through loosely packed glass beads [3,11]. This is interpreted as being due to the shearing stress, which appears inside an elastic molecule, driven close to a hard surface [3]. This shearing stress in combination with the extensional stress, which appears at curved surfaces, leads to stretching of the molecule, thus increasing its contact area and, consequently, the drag on the surface. A detailed study of this mechanism is carried out by Chilcott and Rallison [13], who performed numerical calculations of a flow of a dilute polymer solution, modeled as a suspension of FENE dumbbells, passing cylindrical and spherical surfaces at low Reynolds number. In our case, as a matter of fact, τ_2 accounts to some extent for this stretching deformation as far as it is linked to the gyration radius of the driven polymer, so that probably both effects are simultaneously present in our model and contribute to the observed behavior.

VI. EFFECTIVE DIFFUSIVITY OF A CHAIN DRIVEN THROUGH A POROUS MEDIUM

It appears interesting, following the work of Saffman [27] on the flow of a dynamically neutral material through a porous medium, to study the effective mean square displacement of the center of mass of a driven chain in a moving coordinate system, fixed at the total mass center of all the driven polymers [Eq. (7)], and to calculate by Eq. (10) the longitudinal and transversal components of the diffusion coefficient with respect to the direction of drift.

In the trivial case when no bias is applied, the drift is zero, with only Brownian motion of the chains, and in the new coordinate system one will observe the same displacements as in the conventional absolute coordinate system, so that the effective diffusivity should be the same as the usual diffusion in a system without external fields. In Fig. 12 we demonstrate the behavior of the longitudinal and transversal components of $D_{\rm eff}(t)=g_{3\_\rm c.m.}(t)/t$ for chains of length $N=32$ in a porous medium with $C_{\rm ob}=0.25$ at different bias fields $B=0.063$–0.625. It is evident that at weak fields the two components of the effective diffusivity tend to merge into a single curve close to the curve of the static diffusion without bias. The bias affects the longitudinal component of $D_{\rm eff}$, which after an initial decline rapidly grows with time until saturation is reached, while the transversal component is generally diminished. The gap between both components rapidly opens as the applied bias B exceeds $B_c\approx 0.27$ (note the log-log scale of the graph).

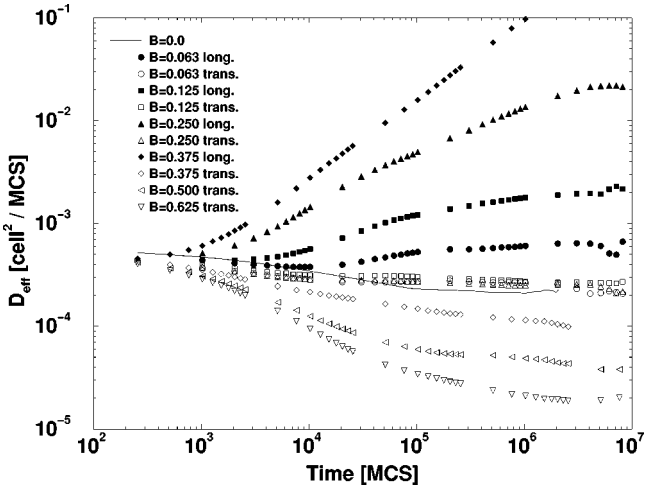

FIG. 12. Log-log plot of longitudinal and transversal effective diffusivity $D_{\rm eff}$ vs time for several values of the bias B. The solid line indicates the diffusion when no bias is applied. Here $N=32$, $C_{\rm ob}=0.25$, and $B_c\approx 0.27$.

This fact reveals in a more direct way the mechanism of reduced mobility of a chain at $B>B_c$. The obstacles, which a driven chain meets in its drift along the bias, are circumvented mainly due to the transversal diffusivity, and when it drops down the chain can hardly go around the obstacles, which leads to rapid decrease of its drift speed. The sharp increase of the longitudinal component means also that the ensemble of polymer chains spreads rapidly in the direction of the drift because some chains are locked for a long time by an obstacle and do not follow the flow while others drift with a great speed until they are hooked again by the host matrix.

The period of initial decline of both components of the effective diffusivity indicates the time scales at which the external field is practically not felt, and the Brownian motion is predominant. It is normal to expect that the length of this period decreases with increase of the bias.

VII. DISCUSSION

In the present investigation we examine the variation of static and dynamic properties of isolated polymer chains driven by a bias field through a quenched environment of randomly distributed obstacles (polymer chains). Both the drift rate and the density of the medium are varied. Our findings agree well with theoretical predictions [2,13–15] and experimental results [3,6,10,11] on the elongation of the polymer conformations in a flow through porous media. Our results indicate that the most probable shape of a chain in such a drift is a hooflike one with both ends pointing in the direction of the drift, as suggested by the observed decrease at high drift rates of the ratio $\langle R_{ee}^2\rangle/\langle R_g^2\rangle$ below its equilibrium value of 6.

We confirm earlier results both by experiment [3,11] and by computer simulations [18,19] of a non-Newtonian flow of the polymer liquid, expressed in an anomalously sharp decrease of the mobility when the bias exceeds some threshold

value. On the grounds of a specific relaxation time, representing the inner mobility of the driven chain, we suggest a simple phenomenological model that fits well to our data on the dynamics of the chains. Basically the model assumes that at low drift rates the interaction of a polymer with an obstacle is like an elastic collision of hard spheres, while at supercritical drift rates the force acting on the driven molecule is high enough to overcome the entropic barrier and press it to the frozen obstacles, which leads to a sharp increase of the capture time.

The model is elucidated by the analysis of the longitudinal and transversal components of the effective diffusivity of the driven chains in a moving coordinate system where the drift motion is eliminated and only Brownian motion still persists. The observed strong decrease of the transversal component of the diffusivity at growing obstacle density makes bypassing of the obstacles extremely slow and thus decreases its overall drift velocity.

ACKNOWLEDGMENTS

This project was supported by EU Grant Copernicus, No. CIPA-CT93-0105 and by the Bulgarian National Science Foundation X-644/1997.

[1] V. Yamakov and A. Milchev, Phys. Rev. E **55**, 1704 (1997).
[2] M. S. Jhon, G. Sekhon, and R. Armstrong, in *Advances in Chemical Physics*, edited by I. Prigogine and S. A. Rice (John Wiley and Sons, New York, 1987), p. 153.
[3] D. F. James and D. R. McLaren, J. Fluid Mech. **70**, 733 (1975).
[4] D. Sigli and M. Coutanceau, J. Non-Newtonian Fluid Mech. **2**, 1 (1977).
[5] R. Cressely and R. Hocquart, Opt. Acta **27**, 699 (1980).
[6] D. F. James and J. H. Saringer, J. Fluid Mech. **97**, 655 (1980).
[7] D. H. King and D. F. James, J. Chem. Phys. **78**, 4749 (1983).
[8] C. Bisgaard, J. Non-Newtonian Fluid Mech. **12**, 283 (1983).
[9] P. N. Dunlap and L. G. Leal, J. Non-Newtonian Fluid Mech. **23**, 5 (1987).
[10] K. Vissmann and H. W. Bewersdorff, J. Non-Newtonian Fluid Mech. **34**, 289 (1990).
[11] C. Chmielewski, C. A. Petty, and K. Jayaraman, J. Non-Newtonian Fluid Mech. **35**, 309 (1990).
[12] O. G. Harlen, J. Non-Newtonian Fluid Mech. **37**, 157 (1990).
[13] M. D. Chilcott and J. M. Rallison, J. Non-Newtonian Fluid Mech. **29**, 381 (1988).
[14] O. G. Harlen, J. M. Rallison, and M. D. Chilcott, J. Non-Newtonian Fluid Mech. **34**, 319 (1990).
[15] E. S. G. Shaqfeh and D. L. Koch, J. Fluid Mech. **244**, 17 (1992).
[16] J. M. Rallison and E. J. Hinch, J. Non-Newtonian Fluid Mech. **29**, 37 (1988).
[17] R. G. Larson, Rheol. Acta **29**, 371 (1990).
[18] R. B. Pandey and J. L. Becklehimer, Phys. Rev. E **51**, 3341 (1995).
[19] G. M. Foo and R. B. Pandey, Phys. Rev. E **51**, 5738 (1995).
[20] W. W. Graessley, Adv. Polym. Sci. **16**, 1 (1974).
[21] M. Doi and S. F. Edwards, in *The Theory of Polymer Dynamics* (Clarendon Press, Oxford, 1986).
[22] G. Ryskin, J. Fluid Mech. **178**, 423 (1987).
[23] I. Gerroff, A. Milchev, W. Paul, and K. Binder, J. Chem. Phys. **98**, 6526 (1993).
[24] A. Milchev, W. Paul, and K. Binder, J. Chem. Phys. **99**, 4786 (1993).
[25] A. Milchev and K. Binder, Macromolecules **29**, 343 (1996); K. Binder, A. Milchev, and J. Baschnagel, Annu. Rev. Mater. Sci. **26**, 107 (1996).
[26] A. Milchev, W. Paul, and K. Binder, Macromol. Theory Simul. **3**, 305 (1994); A. Milchev and K. Binder, J. Phys. II **6**, 21 (1995); J. Comp.-Aided Mat. Des. **2**, 1(1995).
[27] P. G. Saffman, J. Fluid Mech. **6**, 321 (1959).
[28] W. Paul, K. Binder, D. W. Heermann, and K. Kremer, J. Chem. Phys. **95**, 7726 (1991).
[29] A. Keller and J. A. Odell, Colloid Polym. Sci. **263**, 181 (1985).
[30] P. G. de Gennes, *Scaling Concepts in Polymer Physics* (Cornell University Press, Ithaca, NY, 1979).